First Evidence of the $B_s^0 \to K^-\pi^+\gamma$ Decay

R. Aaij *et al.*[*]
(LHCb Collaboration)

(Received 7 January 2026; accepted 9 March 2026; published 30 April 2026)

The first search for the $B_s^0 \to K^-\pi^+\gamma$ decay in the range $796 < m(K^-\pi^+) < 1800$ MeV/c^2 is performed using data from proton-proton collisions collected by the LHCb experiment at center-of-mass energies of 7, 8, and 13 TeV, corresponding to an integrated luminosity of 9 fb^{-1}. The photons are reconstructed through their conversion into an electron-positron pair, which significantly improves the mass resolution of the reconstructed decays with respect to decays with an unconverted photon. A signal excess with a significance of 3.5 standard deviations is measured, constituting the first experimental evidence for this decay. In the range $796 < m(K^-\pi^+) < 996$ MeV/c^2, the ratio $\mathcal{R}$ between the branching fractions of the signal decay and the favored $\overline{B}^0 \to K^-\pi^+\gamma$ decay is measured to be $\mathcal{R} = (3.7 \pm 1.2 \pm 0.4) \times 10^{-2}$ where the first uncertainty is statistical and the second is systematic. This measurement is consistent with the value predicted in the Standard Model. In the range $996 < m(K^-\pi^+) < 1800$ MeV/c^2, the ratio $\mathcal{R} = (0.2 \pm 2.7 \pm 1.3) \times 10^{-2}$ is measured.

DOI: 10.1103/g8fs-djyt

In the Standard Model (SM), $b \to d\gamma$ and $b \to s\gamma$ quark transitions proceed via electroweak loop diagrams. [1] Particles beyond the SM (BSM) of arbitrarily high mass can contribute to these diagrams [2–5]. The $b \to s\gamma$ transition, with amplitude proportional to the Cabibbo-Kobayashi-Maskawa (CKM) matrix element V_{ts}^*, has been measured through several radiative b-hadron decays [6–13]. In contrast, measurements of the $b \to d\gamma$ transition, with amplitude proportional to V_{td}^*, remain limited. Branching fractions ($\mathcal{B}$) of the $B^{+/0} \to \rho(770)^{+/0}\gamma$ and $B^0 \to \omega(782)\gamma$ decays have been measured [14–17] as well as the inclusive branching fraction of $B \to X_d\gamma$ decays [18], where X_d is an unflavored hadronic system.

The ratio of branching fractions between decays mediated by $b \to d\gamma$ and $b \to s\gamma$ transitions can be used to measure $|V_{td}/V_{ts}|$ [19,20]. This value may be compared to determinations based on $B_{(s)}^0$ meson oscillations [21,22] to identify potential contributions from BSM processes. The value of $|V_{td}/V_{ts}|$ extracted from the measured branching fraction ratio $\mathcal{R} \equiv \mathcal{B}(B_s^0 \to \bar{K}^*(892)^0\gamma)/\mathcal{B}(\bar{B}^0 \to \bar{K}^*(892)^0\gamma)$ is theoretically cleaner than determinations using other decays involving $b \to d\gamma$ transitions since dominant uncertainties from the ratios of form factors largely cancel [20]. Using the existing calculations of the form-factor ratio and nonfactorizable effects [20] with updated meson lifetimes, masses, and CKM matrix elements [23–25], the prediction is $\mathcal{R} = (3.9 \pm 0.7) \times 10^{-2}$. However, a new calculation of the form-factor ratio and nonfactorizable effects, incorporating the latest experimental information, will be necessary to reduce the uncertainty on an eventual measurement of $|V_{td}/V_{ts}|$ using $B_s^0 \to \overline{K}^*(892)^0\gamma$ decays.

This Letter reports the first search and first evidence for the $B_s^0 \to K^-\pi^+\gamma$ decay. The reconstructed $K^-\pi^+$ system includes contributions from the $\bar{K}^*(892)^0$ resonance as well as higher-mass states up to 1800 MeV/c^2. Additionally, the ratio of its branching fraction with respect to the $\overline{B}^0 \to K^-\pi^+\gamma$ decay is measured. The analysis uses proton-proton (pp) collision data recorded by the LHCb experiment, corresponding to integrated luminosities of 3 fb^{-1} at center-of-mass energies of 7 and 8 TeV, and 6 fb^{-1} at 13 TeV, referred to as the Run 1 and Run 2 data samples, respectively. In order to avoid experimenter's bias, the data in a mass window within ± 40 MeV/c^2 of the known mass of the B_s^0 meson [25], corresponding to approximately twice the resolution of the signal decay, were not examined until the full procedure had been finalized.

The LHCb detector [26,27] is a single-arm forward spectrometer covering the pseudorapidity range $2 < \eta < 5$. Detector elements include: a silicon-strip vertex detector (VELO) surrounding the pp interaction region [28]; a tracking system, consisting of detectors upstream and downstream of a dipole magnet with a bending power of about 4 T m, that provides a measurement of the momentum, p, of charged particles [29,30]; two ring-imaging Cherenkov (RICH) detectors that are able to discriminate

[*]Full author list given at the end of the Letter.

between different species of charged hadrons [31]; and a calorimeter system able to identify and measure the energy of electrons and photons [32].

The online event selection is performed by a trigger [33,34]. At the hardware trigger stage, events are required to have a muon with high transverse momentum (p_{T}) or a hadron, photon, or electron with high transverse energy (E_{T}) in the calorimeters. The software trigger performs a full event reconstruction and requires that the signal decay candidates contain a secondary vertex consistent with the decay of a b hadron formed of either multiple tracks [35,36] or two high-p_{T} tracks alongside a high-E_{T} photon [37].

Simulation is required to model the effects of the detector resolution and acceptance, and the imposed selection requirements. The pp collisions are generated using PYTHIA [38] with a specific LHCb configuration [39]. Decays of unstable particles are described by EVTGEN [40], in which final-state radiation is generated using PHOTOS [41]. The interaction of the generated particles with the detector, and its response, are implemented using the GEANT4 toolkit [42] as described in Ref. [43]. The simulated samples of B^0, B_s^0, and Λ_b^0 decays are corrected to account for data-simulation differences in the b-hadron production kinematics and detector occupancy using data samples enriched in $\bar{B}^0 \to K^-\pi^+\gamma$, $B_s^0 \to K^+K^-\gamma$, and $\Lambda_b^0 \to pK^-\gamma$ decays, respectively. Particle-identification efficiencies are calibrated using dedicated control samples [44].

Only photons that convert through interactions with the detector material into an electron-positron pair, referred to as *converted photons* [45–47], are used in this search. This improves the mass resolution of the b-hadron candidate by a factor of 3 with respect to candidates formed using photons reconstructed as clusters in the electromagnetic calorimeter (ECAL), reducing the background from the $\bar{B}^0 \to K^-\pi^+\gamma$ decay. Furthermore, the photon trajectory can be matched to the position of the $K^-\pi^+$ combination vertex to reduce background from random combinations of photons and hadrons. Electron candidates are identified among high-p_{T} tracks that are associated with clusters in the ECAL. To mitigate loss in resolution from bremsstrahlung before the magnet, electrons are rejected if an ECAL cluster, identifiable as a photon with $E_{\mathrm{T}} > 75$ MeV, is found at a position consistent with the extrapolation of the electron trajectory. Converted photons are reconstructed in two categories: those that convert early enough that the electrons are reconstructed using the full tracking system (*long* tracks), and those that convert further downstream, where no track segments are formed in the VELO (*downstream* tracks). To reject background from random combinations, the two electron candidates are required to originate from a common vertex, and the mass of the dielectron must be less than 50 MeV/c^2. The photon candidate must have $p_{\mathrm{T}} > 500$ MeV/c and its vertex must be significantly displaced from the primary vertex (PV) that is most consistent with the flight direction of the B candidate, referred to as the associated PV.

To evaluate the contamination to the $\overset{(-)}{B}{}^0_{(s)} \to K^-\pi^+\gamma$ signal decays due to particle misidentification, $B_s^0 \to K^+K^-\gamma$ and $\Lambda_b^0 \to pK^-\gamma$ decays are also analyzed. All of these decay candidates are constructed by combining two high-p_{T} tracks incompatible with originating from any PV and identified using information from the RICH system as pions, kaons, or protons, and requiring that they form a common vertex. The photon candidate is combined with the dihadron pair consistent with originating from the same vertex to form decay candidates that are consistent with originating from a PV. The dihadron masses are required to be in the ranges $796 < m(K^-\pi^+) < 1800$ MeV/c^2, $1000 < m(K^+K^-) < 1800$ MeV/c^2, and $1400 < m(pK^-) < 2500$ MeV/c^2. To reject backgrounds from decays involving a π^0 meson misidentified as a photon, such as the $\overline{B}{}^0 \to [\pi^+\pi^0]_{\rho^+}K^-$ decay, the mass of the combination of the photon assigned the π^0 mass hypothesis with one hadron is required to be greater than 2000 MeV/c^2. Momentum resolution is improved by applying a kinematic fit [48], in which all final-state particles are constrained to originate from the corresponding decay vertex, and the b-hadron candidate is constrained to originate from the associated PV. The mass resolution is further improved by requiring the mass of downstream photon candidates to be below 40 MeV/c^2 and, for candidates containing long electron tracks, the uncertainty on the b-hadron candidate mass to be less than 20 MeV/c^2. These requirements are approximately 85% and 90% efficient on signal decays, respectively.

The data are analyzed separately for the Run 1 and 2 datasets, long and downstream electrons, and low [$796 < m(K^-\pi^+) < 996$ MeV/c^2] and high [$996 < m(K^-\pi^+) < 1800$ MeV/c^2] dihadron mass windows. Separate boosted decision tree (BDT) classifiers [49–51] are trained for each of these categories to further reject background from random combinations of particles. The classifiers are trained using simulated $B_s^0 \to \bar{K}^*(892)^0\gamma$ decays for the signal and $\overset{(-)}{B}{}^0_{(s)} \to K^-\pi^+\gamma$ candidates in data with masses above 5580 MeV/c^2 for the background sample. The classifiers exploit kinematic and topological properties of the decay as well as, for long electron tracks, the amount of charge deposited in the VELO that is larger for converted photons where the two electron tracks overlap, and their compatibility with the electron hypothesis using information from the RICH and calorimeter systems. The requirement on the classifier in the $K^-\pi^+\gamma$ final state is optimized simultaneously with requirements on the kaon and pion-identification probabilities to maximize the figure of merit $\varepsilon_{\mathrm{sig}}/(3/2 + \sqrt{N_{\mathrm{bkg}}})$ [52] for the purpose of finding evidence for this decay. Here, $\varepsilon_{\mathrm{sig}}$ denotes the efficiency of

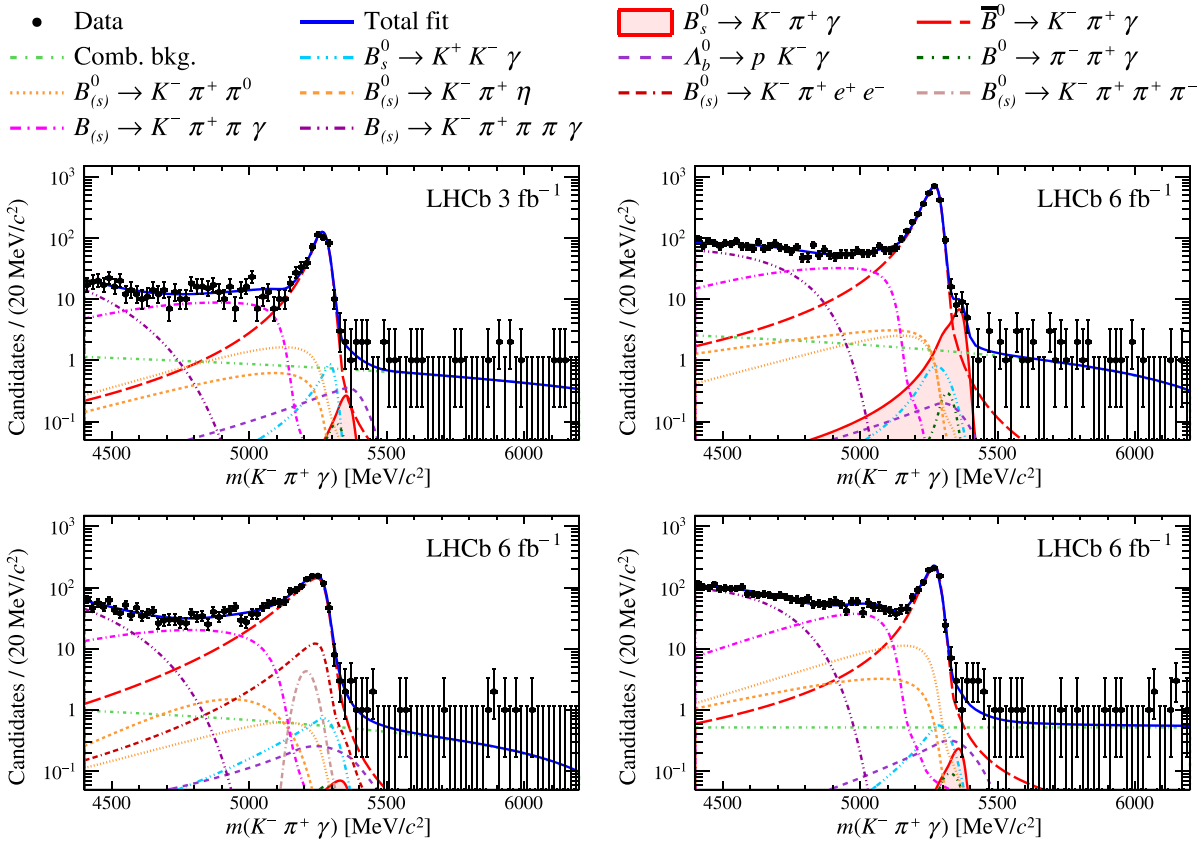

FIG. 1. Mass distribution of selected $K^-\pi^+\gamma$ candidates in (top left) Run 1 downstream low-$m(K^-\pi^+)$ [$796 < m(K^-\pi^+) < 996$ MeV/c^2]; (top right) Run 2 downstream low-$m(K^-\pi^+)$; (bottom left) Run 2 long low-$m(K^-\pi^+)$; and (bottom right) Run 2 downstream high-$m(K^-\pi^+)$ [$996 < m(K^-\pi^+) < 1800$ MeV/c^2] datasets. The model described in the text, fitted separately to each dataset, is also shown. The corresponding measured $B_s^0 \to K^-\pi^+\gamma$ yields are 1 ± 5, 32 ± 11, 2 ± 12, and 0 ± 6, and the measured $\overline{B}^0 \to K^-\pi^+\gamma$ yields are 523 ± 26, 3132 ± 61, 1247 ± 45, and 988 ± 35, where the uncertainties are statistical only.

the selection requirements determined from simulation, and $N_{\rm bkg}$ is the estimated number of candidates from all processes except the signal decay within a mass window corresponding to four times the signal mass resolution, centered on its peak position. The optimal particle identification and BDT requirements correspond to a combinatorial background rejection of at least 95% and a signal efficiency of 55%–98%, where less efficient requirements are necessary for data in $996 < m(K^-\pi^+) < 1800$ MeV/c^2 where signal purity is lower. The same BDT requirement is applied to the $K^+K^-\gamma$ and $pK^-\gamma$ final states without any additional particle-identification criteria.

The best sensitivity to the signal decay is obtained using downstream electrons, which have a smaller probability of bremsstrahlung and therefore better momentum resolution, and in the low-mass window occupied by the $K^*(892)^0$ resonance that offers higher purity. Of the eight available subsets of data, only those with the highest signal-to-background purity in data and mass resolution of the normalization decay are analyzed: low-$m(K^-\pi^+)$ with downstream electrons in Run 1 data; both low- and high-$m(K^-\pi^+)$ with downstream electrons in Run 2 data; and low-$m(K^-\pi^+)$ with long track electrons in Run 2 data. The chosen datasets, established prior to examination of the signal region, each provide an expected signal significance of approximately 1.0 standard deviations or higher assuming the predicted branching fraction; the excluded datasets provide expected significances below 0.3 standard deviations. Figure 1 shows the mass distributions of $K^-\pi^+\gamma$ candidates passing the selection requirements in the datasets with best sensitivity. The signal decay yields are extracted through an extended unbinned maximum-likelihood fit to these data samples.

The $B^{(-)}_{(s)}{}^0 \to K^-\pi^+\gamma$ signal decays are modeled using Johnson S_U (JSU) functions featuring power-law tails on both sides of the peak [53]. For candidates where the downstream tracks are not matched to the correct hits in the tracking detectors, the mass distribution is shifted toward lower values. To account for this effect, a modified Gaussian function with power-law tails on both sides (double-sided Crystal Ball, DSCB) [54] is added to the JSU function. All shape parameters are fixed from simulation, except for the relative fraction of the two

components and deviations of the overall width and peak position from simulation. These are unconstrained and shared between the B^0 and $B_s^0 \to K^-\pi^+\gamma$ decay models.

Partially reconstructed $B \to K^-\pi^+\pi(\pi)\gamma$ decays are modeled with ARGUS functions [55] convolved with the signal model. The endpoints of the ARGUS functions are fixed to the peak position of the signal model reduced by the mass of the missing pions. The other parameters are fixed from simulation, except for the model for two missing pions where the power parameter is free to vary in the fit to data. The yields corresponding to partially reconstructed B^0 and B^+ meson decays are free to vary in the fit to data. To estimate the yields of partially reconstructed B_s^0 meson decays, the $B \to K^-\pi^+\pi(\pi)\gamma$ decay yields are scaled by the ratio of B_s^0 to B meson production cross sections [56] and the branching fraction ratio estimated by applying SU(3) flavor symmetry while accounting for dominant sources of SU(3) breaking.

The $\overset{(-)}{B}{}^0_{(s)} \to K^-\pi^+\pi^0$ and $\overset{(-)}{B}{}^0_{(s)} \to K^-\pi^+\eta$ decays, where one of the two photons from the π^0 or η decay is not reconstructed, are similarly modeled using ARGUS functions convolved with the signal model. The ARGUS endpoint is set to the peak position of the signal model and the shape parameters are fixed from simulation. The yields of such components are fixed relative to that of the $\bar{B}^0 \to K^-\pi^+\gamma$ decay using selection efficiencies from simulation and measured branching fractions, or predictions where measurements are not available [25,57–59]. The yields of $B_s^0 \to K_J^{*0}\eta$ decays ($J = 0,\ 2$), where neither measurements nor predictions are available, are estimated similarly to the yield of $B_s^0 \to K^-\pi^+\pi(\pi)\gamma$ decays.

The $B_s^0 \to K^+K^-\gamma$, $\Lambda_b^0 \to pK^-\gamma$, and $B^0 \to \pi^+\pi^-\gamma$ decays, where one or both hadrons are misidentified, are modeled using DSCB functions with shape parameters fixed from simulation. The yield of $B^0 \to \pi^+\pi^-\gamma$ decays is fixed relative to the yield of $\bar{B}^0 \to K^-\pi^+\gamma$ decays using efficiencies from simulation and the known $B^0 \to \rho(770)^0\gamma$ branching fraction [14], neglecting contributions from higher-mass resonances. The yields of the other misidentified decays are determined using data selected in the $K^+K^-\gamma$ and $pK^-\gamma$ final states, as described in the End Matter.

Finally, $\overset{(-)}{B}{}^0_{(s)} \to \bar{K}^*(892)^0e^+e^-$ and misidentified $\overset{(-)}{B}{}^0_{(s)} \to \bar{K}^*(892)^0\pi^+\pi^-$ decays are modeled using a JSU and a Gaussian function, respectively. The $\bar{B}^0$ decay yields are fixed relative to that of the $\bar{B}^0 \to K^-\pi^+\gamma$ decay using efficiencies from simulation and measured branching fractions [25,60–62]; the yields of the corresponding B_s^0 decays are further scaled using the same method as for $B_s^0 \to K^-\pi^+\pi(\pi)\gamma$ decays. The contamination from $\overset{(-)}{B}{}^0_{(s)} \to \bar{K}^*(892)^0e^+e^-$ and $\overset{(-)}{B}{}^0_{(s)} \to \bar{K}^*(892)^0\pi^+\pi^-$ decays are negligible for downstream electrons. Background from random combinations of particles is modeled using a first-order polynomial function with free slope and yield.

Systematic uncertainties on the signal yield are summarized in Table I. Systematic uncertainties on the yield of the $\bar{B}^0 \to K^-\pi^+\gamma$ decay are calculated similarly. The systematic uncertainty associated with the statistical uncertainty of the $B_s^0 \to K^+K^-\gamma$ and $\Lambda_b^0 \to pK^-\gamma$ decay yields is evaluated as the reduction in the uncertainty of the $B_s^0 \to K^-\pi^+\gamma$ decay yield when those contributions are fixed. All other uncertainties are evaluated from pseudoexperiments generated with an alternative model, taking as the uncertainty the average absolute difference in yield obtained when fitting the baseline model compared to the alternative model. The alternative models are as follows: For $\overset{(-)}{B}{}^0_{(s)} \to K^-\pi^+\gamma$ and $\overset{(-)}{B}{}^0_{(s)} \to \bar{K}^*(892)^0e^+e^-$ decays, and the resolution model for partially reconstructed decays, a

TABLE I. Sources of absolute systematic uncertainty on the signal yield. Three dots indicate contributions that are not relevant for that dataset.

Period	Run 1	Run 2	Run 2	Run 2
Track	downstream	downstream	long	downstream
$m(K^-\pi^+)$	low	low	low	high
Misidentified-hadron yield	0.4	0.5	1.1	1.3
$K^-\pi^+\gamma$ and $\overline{K}^*(892)^0e^+e^-$ model	0.4	1.7	3.0	1.8
$B \to K^-\pi^+\pi\gamma$ resonant structure	<0.1	0.1	0.5	0.2
Misidentified-hadron model	0.4	0.2	0.5	0.9
$\overline{K}^*(892)^0\pi^+\pi^-$ model	...	...	<0.1	...
Combinatorial model	0.1	0.7	1.1	0.1
External inputs	0.2	0.1	0.5	0.3
Simulation sample size	0.4	0.6	0.9	0.4
Hadron-identification corrections	1.6	0.4	0.1	0.9
Electron-identification corrections	...	...	0.1	...
Simulation corrections	0.1	1.7	1.4	0.2
Total	1.9	2.7	3.9	2.6

different width parameter is used for each side of the DSCB function and the JSU function is replaced by a DSCB function. For long-track electrons, the model is evaluated using only reconstructed tracks matched to the correct hits in the tracking detectors. For candidates with downstream electrons, the JSU function is evaluated using only candidates where the photon converts downstream of the VELO and the tracks are matched to the correct hits in the tracking detectors, while the DSCB function is evaluated with the remaining candidates. The model for partially reconstructed $B \to K^-\pi^+\pi\gamma$ decays is evaluated from simulated $B^+ \to K^*(892)^0\pi^+\gamma$ decays. Contributions from decays with misidentified hadrons and $\overset{(-)}{B}{}^0_{(s)} \to \bar{K}^*(892)^0\pi^+\pi^-$ decays are alternatively modeled using bifurcated Gaussian and symmetric DSCB functions, respectively. The combinatorial background is modeled with an exponential function. Branching fractions and b-hadron masses are varied randomly according to their uncertainties in each pseudoexperiment. Where assumptions are made on branching fractions in the absence of predictions or measurements, a 100% uncertainty is assumed. The contamination from $B^0 \to \rho(770)^0\gamma$ decays for $996 < m(K^-\pi^+) < 1800$ MeV$/c^2$ is doubled, and a 100% uncertainty is assigned, to account for missing contributions from heavier resonances. Shape parameters and efficiencies are varied randomly according to their covariance matrices. The uncertainty on the hadron-misidentification corrections includes the size of the calibration sample as well as possible biases introduced by the background subtraction method and variations of the corrections within the phase-space bins in which they are derived. Other simulation corrections, including those related to electron identification, are small and therefore removed.

A yield of 38 ± 18 $B^0_s \to K^-\pi^+\gamma$ decays is measured, where the uncertainty includes both statistical and systematic sources, of which 32 ± 11 correspond to the Run 2 downstream low-$m(K^-\pi^+)$ dataset. Pseudoexperiments show that the probability that background processes can produce a mass distribution that is less compatible with the background-only model than the data, including both statistical and systematic sources of uncertainty, is 2.8×10^{-4}, corresponding to a significance of 3.5 standard deviations.

The signal branching fraction is measured relative to that of the $\bar{B}^0 \to K^-\pi^+\gamma$ decay as

$$\mathcal{R} \equiv \frac{\mathcal{B}(B^0_s \to K^-\pi^+\gamma)}{\mathcal{B}(\bar{B}^0 \to K^-\pi^+\gamma)} = \frac{N(B^0_s \to K^-\pi^+\gamma)}{N(\bar{B}^0 \to K^-\pi^+\gamma)} \frac{\varepsilon(\bar{B}^0 \to K^-\pi^+\gamma)}{\varepsilon(B^0_s \to K^-\pi^+\gamma)} \Big/ \frac{f_s}{f_d},$$

where N are the yields, ε are the efficiencies, and (f_s/f_d) is the ratio of production cross-sections evaluated by weighting the p_{T}-dependent measurement [56] over the simulated p_{T} distribution of $\bar{B}^0 \to K^-\pi^+\gamma$ decays. The ratio of the efficiencies is consistent with unity for all datasets. A correction of 1%–8% is applied for a bias in the measured branching fraction arising from the fit method. It is estimated as the average fit bias observed in pseudoexperiments generated with $\mathcal{R}$ equal to its predicted value.

Systematic uncertainties applied on the normalization of $\mathcal{R}$ are shown in Table II. The uncertainty on the fit bias is the quadrature sum of its statistical uncertainty, the difference in bias between two methods of determining the average, and the variation in the bias value when pseudodatasets are generated with $\mathcal{R}$ equal to its measured value. The uncertainty on the $B^0_{(s)}$ lifetimes [22] and from the simulation sample size are propagated to uncertainties on the efficiency ratio. The uncertainties on the measurement of (f_s/f_d) are propagated to the weighted average value. Correlations between measurements from each dataset arising from the use of common inputs for $B^0_{(s)}$ lifetimes and (f_s/f_d) are considered.

The measured branching fraction ratio is found to be consistent (p-value greater than 0.05) between data corresponding to different $m(K^-\pi^+)$ windows, electron track types, data-taking periods and magnet polarities, and under changes in the selection requirements on the BDT classifier, hadron-identification probabilities, and variables that impact the mass resolution. A simultaneous fit to all datasets with $796 < m(K^-\pi^+) < 996$ MeV$/c^2$, with a common value of $\mathcal{R}$, results in the measurement

TABLE II. Sources of systematic uncertainty on the normalization of the branching fraction ratio in percent.

Period	Run 1	Run 2	Run 2	Run 2
Track	low	low	low	high
$m(K^-\pi^+)$	downstream	downstream	long	downstream
Fit bias	8.8	2.1	3.9	2.4
Lifetime	0.4	0.5	0.4	0.6
Production cross sections	3.2	3.4	3.4	3.4
Simulation sample size	1.6	1.5	2.3	1.5
Total	9.5	4.3	5.7	4.5

$$\mathcal{R}_{\text{low}} = (3.7 \pm 1.2 \pm 0.4) \times 10^{-2}$$
$$\text{for } 796 < m(K^-\pi^+) < 996 \text{ MeV}/c^2,$$

where the first uncertainty is statistical and the second systematic, which is in excellent agreement with the SM prediction. Additionally, the ratio

$$\mathcal{R}_{\text{high}} = (0.2 \pm 2.7 \pm 1.3) \times 10^{-2}$$
$$\text{for } 996 < m(K^-\pi^+) < 1800 \text{ MeV}/c^2,$$

is measured. Correlations between the two measurements are negligible.

In summary, a search for the rare $B_s^0 \to K^-\pi^+\gamma$ decay is performed using pp collision data corresponding to an integrated luminosity of 9 fb^{-1}. An excess of events is found with a significance of 3.5 standard deviations, which constitutes the first evidence for this decay. Updated theoretical inputs will permit a test of the SM using the measured branching fraction ratio. Large improvements in precision are anticipated with the new dataset being collected by the upgraded LHCb detector [63].

We are indebted to the communities behind the multiple open-source software packages on which we depend.

Acknowledgments—We express our gratitude to our colleagues in the CERN accelerator departments for the excellent performance of the LHC. We thank the technical and administrative staff at the LHCb institutes. We acknowledge support from CERN and from the national agencies: ARC (Australia); CAPES, CNPq, FAPERJ and FINEP (Brazil); MOST and NSFC (China); CNRS/IN2P3 (France); BMFTR, DFG and MPG (Germany); INFN (Italy); NWO (Netherlands); MNiSW and NCN (Poland); MCID/IFA (Romania); MICIU and AEI (Spain); SNSF and SER (Switzerland); NASU (Ukraine); STFC (United Kingdom); DOE NP and NSF (USA). We acknowledge the computing resources that are provided by ARDC (Australia), CBPF (Brazil), CERN, IHEP, and LZU (China), IN2P3 (France), KIT, and DESY (Germany), INFN (Italy), SURF (Netherlands), Polish WLCG (Poland), IFIN-HH (Romania), PIC (Spain), CSCS (Switzerland), and GridPP (United Kingdom). Individual groups or members have received support from Key Research Program of Frontier Sciences of CAS, CAS PIFI, CAS CCEPP, Minciencias (Colombia); EPLANET, Marie Skłodowska-Curie Actions, ERC, and NextGenerationEU (European Union); A*MIDEX, ANR, IPhU, and Labex P2IO, and Région Auvergne-Rhône-Alpes (France); Alexander-von-Humboldt Foundation (Germany); ICSC (Italy); Severo Ochoa and María de Maeztu Units of Excellence, GVA, XuntaGal, GENCAT, InTalent-Inditex, and Prog. Atracción Talento CM (Spain); SRC (Sweden); the Leverhulme Trust, the Royal Society, and UKRI (United Kingdom).

Data availability—The data that support the findings of this article are openly available [66].

[1] The inclusion of charge-conjugate processes is implied throughout this Letter.
[2] X.-Q. Li, Y.-D. Yang, and X.-B. Yuan, Exclusive radiative B-meson decays within minimal flavor-violating two-Higgs-doublet models, Phys. Rev. D **89**, 054024 (2014).
[3] Z. Xiao and C. Zhuang, Exclusive $B \to (K^*, \rho)\gamma$ decays in the general two Higgs doublet models, Eur. Phys. J. C **33**, 349 (2004).
[4] A. Ali and E. Lunghi, Implications of $B \to \rho\gamma$ measurements in the standard model and supersymmetric theories, Eur. Phys. J. C **26**, 195 (2002).
[5] A. Arhrib, C.-K. Chua, and W.-S. Hou, Supersymmetric model contributions to $B_d^0 - \bar{B}_d^0$ mixing and $B \to \pi\pi$, $\rho\gamma$ decays, Eur. Phys. J. C **21**, 567 (2001).
[6] R. Aaij *et al.* (LHCb Collaboration), Measurement of CP-violating and mixing-induced observables in $B_s^0 \to \phi\gamma$ decays, Phys. Rev. Lett. **123**, 081802 (2019).
[7] R. Aaij *et al.* (LHCb Collaboration), Measurement of the photon polarization in $\Lambda_b^0 \to \Lambda\gamma$ decays, Phys. Rev. D **105**, 051104 (2022).
[8] R. Aaij *et al.* (LHCb Collaboration), Strong constraints on the $b \to s\gamma$ photon polarisation from $B^0 \to K^{*0}e^+e^-$ decays, J. High Energy Phys. 12 (2020) 081.
[9] R. Aaij *et al.* (LHCb Collaboration), Constraints on the photon polarisation in $b \to s\gamma$ transitions using $B_s^0 \to \phi e^+e^-$ decays, J. High Energy Phys. 03 (2025) 047.
[10] R. Aaij *et al.* (LHCb Collaboration), Measurement of the ratio of branching fractions $\mathcal{B}(B^0 \to K^{*0}\gamma)/\mathcal{B}(B_s^0 \to \phi\gamma)$ and the direct CP asymmetry in $B^0 \to K^{*0}\gamma$, Nucl. Phys. **B867**, 1 (2013).
[11] I. Adachi *et al.* (Belle II Collaboration), Measurement of $B \to K^*(892)\gamma$ decays at Belle II, J. High Energy Phys. 09 (2025) 024.
[12] P. del Amo Sanchez *et al.* (*BABAR* Collaboration), Time-dependent analysis of $B^0 \to K_S^0\pi^-\pi^+\gamma$ decays and studies of the $K^+\pi^-\pi^+$ system in $B^+ \to K^+\pi^-\pi^+\gamma$ decays, Phys. Rev. D **93**, 052013 (2016).
[13] A. Paul and D. M. Straub, Constraints on new physics from radiative B decays, J. High Energy Phys. 04 (2017) 027.
[14] R. Aaij *et al.* (LHCb Collaboration), Measurement of the $B^0 \to \rho^0\gamma$ branching fraction, J. High Energy Phys. 12 (2025) 151.
[15] I. Adachi *et al.* (Belle Collaboration and Belle II Collaboration), Measurement of branching fractions, CP asymmetry, and isospin asymmetry for $B \to \rho\gamma$ decays using Belle and Belle II data, Phys. Rev. D **111**, L071103 (2025).
[16] N. Taniguchi *et al.* (Belle Collaboration), Measurement of branching fractions, isospin and CP-violating asymmetries for exclusive $b \to d\gamma$ modes, Phys. Rev. Lett. **101**, 111801 (2008); **101**, 129904(E) (2008).
[17] B. Aubert *et al.* (*BABAR* Collaboration), Measurements of branching fractions for $B^+ \to \rho^+\gamma$, $B^0 \to \rho^0\gamma$, and $B^0 \to \omega\gamma$, Phys. Rev. D **78**, 112001 (2008).
[18] P. del Amo Sanchez *et al.* (*BABAR* Collaboration), Study of $B \to X\gamma$ decays and determination of $|V_{td}/V_{ts}|$, Phys. Rev. D **82**, 051101 (2010).
[19] P. Ball and R. Zwicky, $|V_{td}/V_{ts}|$ from $B \to V\gamma$, J. High Energy Phys. 04 (2006) 046.
[20] P. Ball, G. W. Jones, and R. Zwicky, $B \to V\gamma$ beyond QCD factorisation, Phys. Rev. D **75**, 054004 (2007).

[21] R. Aaij *et al.* (LHCb Collaboration), Precise determination of the $B_s^0 - \bar{B}_s^0$ oscillation frequency, Nat. Phys. **18**, 1 (2022).

[22] S. Banerjee *et al.* (Heavy Flavor Averaging Group), Averages of b-hadron, c-hadron, and τ-lepton properties as of 2023, Phys. Rev. D **113**, 012008 (2026), updated results and plots available at https://hflav.web.cern.ch.

[23] J. Charles *et al.* (CKMfitter group), *CP* violation and the CKM matrix: Assessing the impact of the asymmetric B factories, Eur. Phys. J. C **41**, 1 (2005).

[24] J. Charles *et al.* (CKMfitter group), Current status of the standard model CKM fit and constraints on $\Delta F = 2$ new physics, Phys. Rev. D **91**, 073007 (2015).

[25] S. Navas *et al.* (Particle Data Group), Review of particle physics, Phys. Rev. D **110**, 030001 (2024).

[26] A. A. Alves Jr. *et al.* (LHCb Collaboration), The LHCb detector at the LHC, J. Instrum. **3**, S08005 (2008).

[27] R. Aaij *et al.* (LHCb Collaboration), LHCb detector performance, Int. J. Mod. Phys. A **30**, 1530022 (2015).

[28] R. Aaij *et al.*, Performance of the LHCb vertex locator, J. Instrum. **9**, P09007 (2014).

[29] R. Arink *et al.*, Performance of the LHCb outer tracker, J. Instrum. **9**, P01002 (2014).

[30] P. d'Argent *et al.*, Improved performance of the LHCb outer tracker in LHC Run 2, J. Instrum. **12**, P11016 (2017).

[31] M. Adinolfi *et al.*, Performance of the LHCb RICH detector at the LHC, Eur. Phys. J. C **73**, 2431 (2013).

[32] C. Abellán Beteta *et al.*, Calibration and performance of the LHCb calorimeters in Run 1 and 2 at the LHC, arXiv:2008.11556.

[33] R. Aaij *et al.*, The LHCb trigger and its performance in 2011, J. Instrum. **8**, P04022 (2013).

[34] R. Aaij *et al.*, Design and performance of the LHCb trigger and full real-time reconstruction in Run 2 of the LHC, J. Instrum. **14**, P04013 (2019).

[35] V. V. Gligorov and M. Williams, Efficient, reliable and fast high-level triggering using a bonsai boosted decision tree, J. Instrum. **8**, P02013 (2013).

[36] T. Likhomanenko, P. Ilten, E. Khairullin, A. Rogozhnikov, A. Ustyuzhanin, and M. Williams, LHCb topological trigger reoptimization, J. Phys. Conf. Ser. **664**, 082025 (2015).

[37] A. Puig, The HLT2 radiative topological lines, CERN, LHCb-PUB-2012-002, CERN-LHCb-PUB-2012-002, 2012.

[38] T. Sjöstrand, S. Mrenna, and P. Skands, A brief introduction to PYTHIA 8.1, Comput. Phys. Commun. **178**, 852 (2008); PYTHIA 6.4 physics and manual, J. High Energy Phys. 05 (2006) 026.

[39] I. Belyaev *et al.*, Handling of the generation of primary events in Gauss, the LHCb simulation framework, J. Phys. Conf. Ser. **331**, 032047 (2011).

[40] D. J. Lange, The EvtGen particle decay simulation package, Nucl. Instrum. Methods Phys. Res., Sect. A **462**, 152 (2001).

[41] N. Davidson, T. Przedzinski, and Z. Was, PHOTOS interface in C++: Technical and physics documentation, Comput. Phys. Commun. **199**, 86 (2016).

[42] J. Allison *et al.* (Geant4 Collaboration), Geant4 developments and applications, IEEE Trans. Nucl. Sci. **53** (2006) 270; Geant4: A simulation toolkit, Nucl. Instrum. Methods Phys. Res., Sect. A **506** (2003) 250.

[43] M. Clemencic, G. Corti, S. Easo, C. R. Jones, S. Miglioranzi, M. Pappagallo, and P. Robbe, The LHCb simulation application, Gauss: Design, evolution and experience, J. Phys. Conf. Ser. **331**, 032023 (2011).

[44] R. Aaij *et al.*, Selection and processing of calibration samples to measure the particle identification performance of the LHCb experiment in Run 2, Eur. Phys. J. Tech. Instrum. **6**, 1 (2019).

[45] R. Aaij *et al.* (LHCb Collaboration), Measurement of the relative rate of prompt χ_{c0}, χ_{c1} and χ_{c2} production at $\sqrt{s} = 7$ TeV, J. High Energy Phys. 10 (2013) 115.

[46] R. Aaij *et al.* (LHCb Collaboration), Measurement of the $\chi_b(3P)$ mass and of the relative rate of $\chi_{b1}(1P)$ and $\chi_{b2}(1P)$ production, J. High Energy Phys. 10 (2014) 088.

[47] R. Aaij *et al.* (LHCb Collaboration), Search for the decays $B^0 \to J/\psi\gamma$ and $B_s^0 \to J/\psi\gamma$, Phys. Rev. D **92**, 112002 (2015).

[48] W. D. Hulsbergen, Decay chain fitting with a Kalman filter, Nucl. Instrum. Methods Phys. Res., Sect. A **552**, 566 (2005).

[49] L. Breiman, J. H. Friedman, R. A. Olshen, and C. J. Stone, *Classification and Regression Trees* (Wadsworth International Group, Belmont, CA, 1984).

[50] Y. Freund and R. E. Schapire, A decision-theoretic generalization of on-line learning and an application to boosting, J. Comput. Syst. Sci. **55**, 119 (1997).

[51] H. Voss, A. Hoecker, J. Stelzer, and F. Tegenfeldt, TMVA—Toolkit for Multivariate Data Analysis with ROOT, Proc. Sci. ACAT2007 (**2007**) 040; A. Hoecker *et al.*, TMVA 4—Toolkit for Multivariate Data Analysis with ROOT. Users Guide, arXiv:physics/0703039.

[52] G. Punzi, Sensitivity of searches for new signals and its optimization, eConf **C030908**, MODT002 (2003).

[53] N. L. Johnson, Systems of frequency curves generated by methods of translation, Biometrika **36**, 149 (1949).

[54] T. Skwarnicki, A study of the radiative cascade transitions between the Upsilon-prime and Upsilon resonances, Ph.D. thesis, Institute of Nuclear Physics, Krakow, 1986, DESY-F31-86-02.

[55] H. Albrecht *et al.* (ARGUS Collaboration), Search for hadronic $b \to u$ decays, Phys. Lett. B **241**, 278 (1990).

[56] R. Aaij *et al.* (LHCb Collaboration), Precise measurement of the f_s/f_d ratio of fragmentation fractions and of B_s^0 decay branching fractions, Phys. Rev. D **104**, 032005 (2021).

[57] J. P. Lees *et al.* (*BABAR* Collaboration), Amplitude analysis of $B^0 \to K^+\pi^-\pi^0$ and evidence of direct *CP* violation in $B \to K^*\pi$ decays, Phys. Rev. D **83**, 112010 (2011).

[58] S.-H. Zhou, X.-X. Hai, R.-H. Li, and C.-D. Lu, Analysis of three-body charmless B-meson decays under the factorization-assisted topological-amplitude approach, Phys. Rev. D **107**, 116023 (2023).

[59] W.-F. Wang, J. Chai, and A.-J. Ma, Contributions of $K_0^*(1430)$ and $K_0^*(1950)$ in the three-body decays $B \to K\pi h$, J. High Energy Phys. 03 (2020) 162.

[60] J.-T. Wei *et al.* (Belle Collaboration), Measurement of the differential branching fraction and forward-backward asymmetry for $B \to K^{(*)}\ell^+\ell^-$, Phys. Rev. Lett. **103**, 171801 (2009).

[61] B. Aubert *et al.* (*BABAR* Collaboration), Direct *CP*, lepton flavor and isospin asymmetries in the decays $B \to K^{(*)}\ell^+\ell^-$, Phys. Rev. Lett. **102**, 091803 (2009).

[62] B. Aubert *et al.* (*BABAR* Collaboration), Measurements of the branching fractions of $B^0 \to K^{*0}K^+K^-$, $B^0 \to K^{*0}\pi^+K^-$, $B^0 \to K^{*0}K^+\pi^-$, and $B^0 \to K^{*0}\pi^+\pi^-$, Phys. Rev. D **76**, 071104 (2007).

[63] R. Aaij *et al.* (LHCb Collaboration), The LHCb Upgrade I, J. Instrum. **19**, P05065 (2024).
[64] R. Aaij *et al.* (LHCb Collaboration), Amplitude analysis of the radiative decay $B_s^0 \to K^+K^-\gamma$, J. High Energy Phys. 08 (2024) 093.
[65] R. Aaij *et al.* (LHCb Collaboration), Amplitude analysis of the $\Lambda_b^0 \to pK^-\gamma$ decay, J. High Energy Phys. 06 (2024) 098.
[66] R. Aaij *et al.* (LHCb Collaboration), First evidence of the $B_s^0 \to K^-\pi^+\gamma$ decay (2026), https://cds.cern.ch/record/2951968.

End Matter

The yields of $B_s^0 \to K^+K^-\gamma$ and $\Lambda_b^0 \to pK^-\gamma$ decays misidentified as $K^-\pi^+\gamma$ candidates are evaluated using an extended unbinned maximum-likelihood fit performed simultaneously with the $K^-\pi^+\gamma$, $K^+K^-\gamma$, and $pK^-\gamma$ final states. To reduce the dependence of the misidentified yield evaluation on the dihadron spectrum of these decays, the requirements on $m(K^-\pi^+)$ are also applied on the invariant mass of the K^+K^- and pK^-

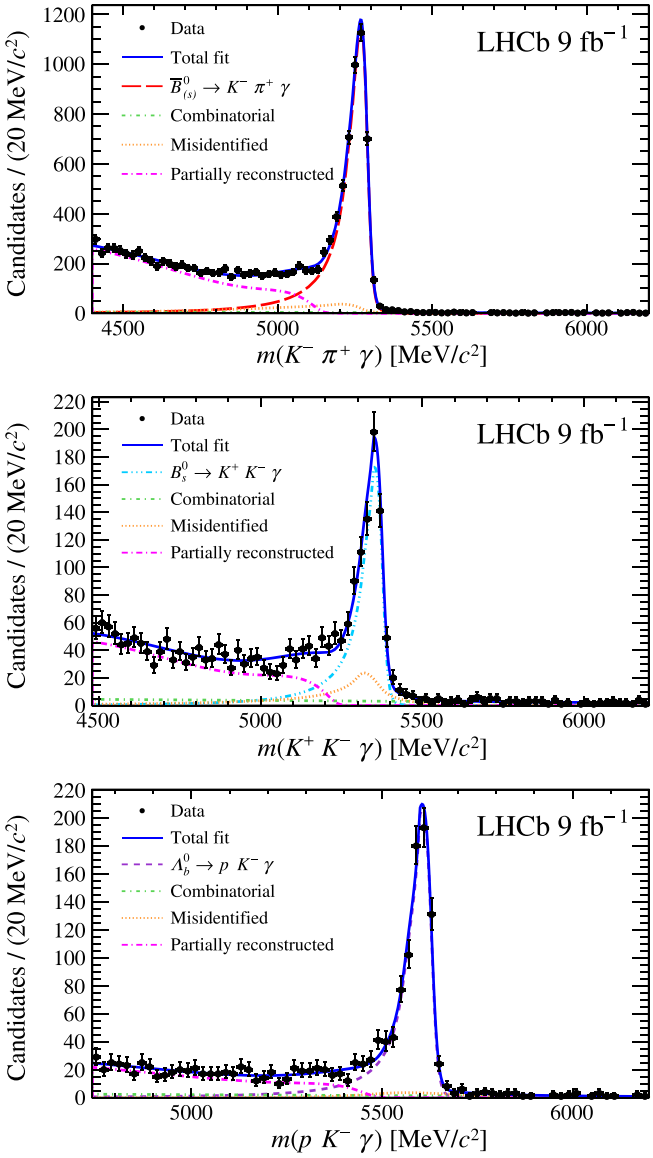

FIG. 2. Mass distribution of selected (top) $B^{(-)}_{(s)}{}^0 \to K^-\pi^+\gamma$, (middle) $B_s^0 \to K^+K^-\gamma$, and (bottom) $\Lambda_b^0 \to pK^-\gamma$ candidates, obtained by summing the four data samples considered in the analysis. The solid curve represents the sum of the fit functions from the individual samples, as described in the text. To improve visibility, the fit functions for sources of misidentified ($\overline{B}{}^0 \to K^-\pi^+\gamma$, $B_s^0 \to K^+K^-\gamma$, $\Lambda_b^0 \to pK^-\gamma$, $B^0_{(s)} \to K^-\pi^+\pi^0$, $B^0_{(s)} \to K^-\pi^+\eta$, $B^0_{(s)} \to K^-\pi^+e^+e^-$, $B^0_{(s)} \to K^-\pi^+\pi^-\pi^+$) and partially reconstructed [$B_{(s)} \to K^-\pi^+\pi(\pi)\gamma$] backgrounds have been summed.

combinations when the pion mass hypothesis is applied to one of the kaons in the $B_s^0 \to K^+K^-\gamma$ decay or to the proton. The yields of the misidentified decays are parametrized as their yield measured in the correct final states multiplied by the selection efficiency ratio. Selection efficiencies are derived using simulated samples of $H_b \to [K^-h^+]_X\gamma$ decays, where H_b is a b-hadron, h^+ is a charged pion, kaon, or proton, and X denotes a resonant state with a large fit fraction. The efficiencies for the $\bar{B}^0 \to [K^-\pi^+]_X\gamma$ and $B_s^0 \to [K^+K^-]_X\gamma$ decays are evaluated as weighted averages of all considered resonant states, where the efficiency for each decay mode is weighted by its fit fraction [25,64]. The uncertainties on the fit fractions are enlarged by the deviation of the summed fit fractions from unity to account for nonresonant, interference, and neglected contributions. Since the $\Lambda_b^0 \to [pK^-]_X\gamma$ decay includes a very large number of interfering resonances [65], four resonances of different masses are considered and each assigned equal weight in the average. When evaluating the systematic uncertainties associated with external inputs, pseudoexperiments are generated using an alternative model that includes only one of the four resonances in turn. Figure 2 shows the invariant-mass distribution of candidates selected in each of the three final states summed over the four analyzed datasets, as well as the summed fit models.

R. Aaij,[38] A. S. W. Abdelmotteleb,[58] C. Abellan Beteta,[52] F. Abudinén,[60] T. Ackernley,[62] A. A. Adefisoye,[70] B. Adeva,[48] M. Adinolfi,[56] P. Adlarson,[86] C. Agapopoulou,[14] C. A. Aidala,[88] Z. Ajaltouni,[11] S. Akar,[11] K. Akiba,[38] M. Akthar,[40] P. Albicocco,[28] J. Albrecht,[19,a] R. Aleksiejunas,[82] F. Alessio,[50] P. Alvarez Cartelle,[57,48] R. Amalric,[16] S. Amato,[3] J. L. Amey,[56] Y. Amhis,[14] L. An,[6] L. Anderlini,[27] M. Andersson,[52] P. Andreola,[52] M. Andreotti,[26] S. Andres Estrada,[45] A. Anelli,[31,b] D. Ao,[7] C. Arata,[12] F. Archilli,[37] Z. Areg,[70] M. Argenton,[26] S. Arguedas Cuendis,[9,50] L. Arnone,[31,b] A. Artamonov,[44] M. Artuso,[70] E. Aslanides,[13] R. Ataíde Da Silva,[51] M. Atzeni,[66] B. Audurier,[12] J. A. Authier,[15] D. Bacher,[65] I. Bachiller Perea,[51] S. Bachmann,[22] M. Bachmayer,[51] J. J. Back,[58] P. Baladron Rodriguez,[48] V. Balagura,[15] A. Balboni,[26] W. Baldini,[26] Z. Baldwin,[80] L. Balzani,[19] H. Bao,[7] J. Baptista de Souza Leite,[2] C. Barbero Pretel,[48,12] M. Barbetti,[27] I. R. Barbosa,[71] R. J. Barlow,[64] M. Barnyakov,[25] S. Barsuk,[14] W. Barter,[60] J. Bartz,[70] S. Bashir,[40] B. Batsukh,[5] P. B. Battista,[14] A. Bavarchee,[81] A. Bay,[51] A. Beck,[66] M. Becker,[19] F. Bedeschi,[35] I. B. Bediaga,[2] N. A. Behling,[19] S. Belin,[48] A. Bellavista,[25] K. Belous,[44] I. Belov,[29] I. Belyaev,[36] G. Benane,[13] G. Bencivenni,[28] E. Ben-Haim,[16] A. Berezhnoy,[44] R. Bernet,[52] S. Bernet Andres,[47] A. Bertolin,[33] F. Betti,[60] J. Bex,[57] O. Bezshyyko,[87] S. Bhattacharya,[81] M. S. Bieker,[18] N. V. Biesuz,[26] A. Biolchini,[38] M. Birch,[63] F. C. R. Bishop,[10] A. Bitadze,[64] A. Bizzeti,[27,c] T. Blake,[58,d] F. Blanc,[51] J. E. Blank,[19] S. Blusk,[70] V. Bocharnikov,[44] J. A. Boelhauve,[19] O. Boente Garcia,[50] T. Boettcher,[89] A. Bohare,[60] A. Boldyrev,[44] C. Bolognani,[84] R. Bolzonella,[26,e] R. B. Bonacci,[1] N. Bondar,[44,50] A. Bordelius,[50] F. Borgato,[33,50] S. Borghi,[64] M. Borsato,[31,b] J. T. Borsuk,[85] E. Bottalico,[62] S. A. Bouchiba,[51] M. Bovill,[65] T. J. V. Bowcock,[62] A. Boyer,[50] C. Bozzi,[26] J. D. Brandenburg,[90] A. Brea Rodriguez,[51] N. Breer,[19] J. Brodzicka,[41] J. Brown,[62] D. Brundu,[32] E. Buchanan,[60] M. Burgos Marcos,[84] C. Burr,[50] C. Buti,[27] J. S. Butter,[57] J. Buytaert,[50] W. Byczynski,[50] S. Cadeddu,[32] H. Cai,[76] Y. Cai,[5] A. Caillet,[16] R. Calabrese,[26,e] L. Calefice,[46] M. Calvi,[31,b] M. Calvo Gomez,[47] P. Camargo Magalhaes,[2,f] J. I. Cambon Bouzas,[48] P. Campana,[28] A. C. Campos,[3] A. F. Campoverde Quezada,[7] S. Capelli,[31] M. Caporale,[25] L. Capriotti,[26] R. Caravaca-Mora,[9] A. Carbone,[25,g] L. Carcedo Salgado,[48] R. Cardinale,[29,h] A. Cardini,[32] P. Carniti,[31] L. Carus,[22] A. Casais Vidal,[66] R. Caspary,[22] G. Casse,[62] M. Cattaneo,[50] G. Cavallero,[26] V. Cavallini,[26,e] S. Celani,[50] I. Celestino,[35,i] S. Cesare,[50,j] A. J. Chadwick,[62] I. Chahrour,[88] H. Chang,[4,k] M. Charles,[16] Ph. Charpentier,[50] E. Chatzianagnostou,[38] R. Cheaib,[81] M. Chefdeville,[10] C. Chen,[57] J. Chen,[51] S. Chen,[5] Z. Chen,[7] A. Chen Hu,[63] M. Cherif,[12] A. Chernov,[41] S. Chernyshenko,[54] X. Chiotopoulos,[84] V. Chobanova,[45] M. Chrzaszcz,[41] A. Chubykin,[44] V. Chulikov,[28,36,50] P. Ciambrone,[28] X. Cid Vidal,[48] G. Ciezarek,[50] P. Cifra,[38] P. E. L. Clarke,[60] M. Clemencic,[50] H. V. Cliff,[57] J. Closier,[50] C. Cocha Toapaxi,[22] V. Coco,[50] J. Cogan,[13] E. Cogneras,[11] L. Cojocariu,[43] S. Collaviti,[51] P. Collins,[50] T. Colombo,[50] M. Colonna,[19] A. Comerma-Montells,[46] L. Congedo,[24] J. Connaughton,[58] A. Contu,[32] N. Cooke,[61] G. Cordova,[35,i] C. Coronel,[67] I. Corredoira,[12] A. Correia,[16] G. Corti,[50] J. Cottee Meldrum,[56] B. Couturier,[50]

D. C. Craik,[52] M. Cruz Torres,[2,l] M. Cubero Campos,[9] E. Curras Rivera,[51] R. Currie,[60] C. L. Da Silva,[69] S. Dadabaev,[44] X. Dai,[4] E. Dall'Occo,[50] J. Dalseno,[45] C. D'Ambrosio,[63] J. Daniel,[11] G. Darze,[3] A. Davidson,[58] J. E. Davies,[64] O. De Aguiar Francisco,[64] C. De Angelis,[32,m] F. De Benedetti,[50] J. de Boer,[38] K. De Bruyn,[83] S. De Capua,[64] M. De Cian,[64,50] U. De Freitas Carneiro Da Graca,[2,n] E. De Lucia,[28] J. M. De Miranda,[2] L. De Paula,[3] M. De Serio,[24,o] P. De Simone,[28] F. De Vellis,[19] J. A. de Vries,[84] F. Debernardis,[24] D. Decamp,[10] S. Dekkers,[1] L. Del Buono,[16] B. Delaney,[66] J. Deng,[8] V. Denysenko,[52] O. Deschamps,[11] F. Dettori,[32,m] B. Dey,[81] P. Di Nezza,[28] I. Diachkov,[44] S. Didenko,[44] S. Ding,[70] Y. Ding,[51] L. Dittmann,[22] V. Dobishuk,[54] A. D. Docheva,[61] A. Doheny,[58] C. Dong,[4,k] F. Dordei,[32] A. C. dos Reis,[2] A. D. Dowling,[70] L. Dreyfus,[13] W. Duan,[74] P. Duda,[85] L. Dufour,[51] V. Duk,[34] P. Durante,[50] M. M. Duras,[85] J. M. Durham,[69] O. D. Durmus,[81] A. Dziurda,[41] A. Dzyuba,[44] S. Easo,[59] E. Eckstein,[18] U. Egede,[1] A. Egorychev,[44] V. Egorychev,[44] S. Eisenhardt,[60] E. Ejopu,[62] L. Eklund,[86] M. Elashri,[67] D. Elizondo Blanco,[9] J. Ellbracht,[19] S. Ely,[63] A. Ene,[43] J. Eschle,[70] T. Evans,[38] F. Fabiano,[14] S. Faghih,[67] L. N. Falcao,[31,b] B. Fang,[7] R. Fantechi,[35] L. Fantini,[34,p] M. Faria,[51] K. Farmer,[60] F. Fassin,[83,38] D. Fazzini,[31,b] L. Felkowski,[85] M. Feng,[5,7] A. Fernandez Casani,[49] M. Fernandez Gomez,[48] A. D. Fernez,[68] F. Ferrari,[25,g] F. Ferreira Rodrigues,[3] M. Ferrillo,[52] M. Ferro-Luzzi,[50] S. Filippov,[44] R. A. Fini,[24] M. Fiorini,[26,e] M. Firlej,[40] K. L. Fischer,[65] D. S. Fitzgerald,[88] C. Fitzpatrick,[64] T. Fiutowski,[40] F. Fleuret,[15] A. Fomin,[53] M. Fontana,[25,50] L. A. Foreman,[64] R. Forty,[50] D. Foulds-Holt,[60] V. Franco Lima,[3] M. Franco Sevilla,[68] M. Frank,[50] E. Franzoso,[26,e] G. Frau,[64] C. Frei,[50] D. A. Friday,[64,50] J. Fu,[7] Q. Führing,[19,57,a] T. Fulghesu,[13] G. Galati,[24,o] M. D. Galati,[38] A. Gallas Torreira,[48] D. Galli,[25,g] S. Gambetta,[60] M. Gandelman,[3] P. Gandini,[30] B. Ganie,[64] H. Gao,[7] R. Gao,[65] T. Q. Gao,[57] Y. Gao,[8] Y. Gao,[6] Y. Gao,[8] L. M. Garcia Martin,[51] P. Garcia Moreno,[46] J. García Pardiñas,[66] P. Gardner,[68] L. Garrido,[46] C. Gaspar,[50] A. Gavrikov,[33] L. L. Gerken,[19] E. Gersabeck,[20] M. Gersabeck,[20] T. Gershon,[58] S. Ghizzo,[29,h] Z. Ghorbanimoghaddam,[56] F. I. Giasemis,[16,q] V. Gibson,[57] H. K. Giemza,[42] A. L. Gilman,[67] M. Giovannetti,[28] A. Gioventù,[46] L. Girardey,[64,59] M. A. Giza,[41] F. C. Glaser,[22,14] V. V. Gligorov,[16] C. Göbel,[71] L. Golinka-Bezshyyko,[87] E. Golobardes,[47] D. Golubkov,[44] A. Golutvin,[63,50] S. Gomez Fernandez,[46] W. Gomulka,[40] I. Gonçales Vaz,[50] F. Goncalves Abrantes,[65] M. Goncerz,[41] G. Gong,[4,k] J. A. Gooding,[19] I. V. Gorelov,[44] C. Gotti,[31] E. Govorkova,[66] J. P. Grabowski,[30] L. A. Granado Cardoso,[50] E. Graugés,[46] E. Graverini,[35,51] L. Grazette,[58] G. Graziani,[27] A. T. Grecu,[43] N. A. Grieser,[67] L. Grillo,[61] S. Gromov,[44] C. Gu,[15] M. Guarise,[26] L. Guerry,[11] A.-K. Guseinov,[51] E. Gushchin,[44] Y. Guz,[6,50] T. Gys,[50] K. Habermann,[18] T. Hadavizadeh,[1] C. Hadjivasiliou,[68] G. Haefeli,[51] C. Haen,[50] S. Haken,[57] G. Hallett,[58] P. M. Hamilton,[68] J. Hammerich,[62] Q. Han,[33] X. Han,[22,50] S. Hansmann-Menzemer,[22] L. Hao,[7] N. Harnew,[65] T. H. Harris,[1] M. Hartmann,[14] S. Hashmi,[40] J. He,[7,r] N. Heatley,[14] A. Hedes,[64] F. Hemmer,[50] C. Henderson,[67] R. Henderson,[14] R. D. L. Henderson,[1] A. M. Hennequin,[50] K. Hennessy,[62] L. Henry,[51] J. Herd,[63] P. Herrero Gascon,[22] J. Heuel,[17] A. Heyn,[13] A. Hicheur,[3] G. Hijano Mendizabal,[52] J. Horswill,[64] R. Hou,[8] Y. Hou,[11] D. C. Houston,[61] N. Howarth,[62] W. Hu,[7] X. Hu,[4] W. Hulsbergen,[38] R. J. Hunter,[58] M. Hushchyn,[44] D. Hutchcroft,[62] M. Idzik,[40] D. Ilin,[44] P. Ilten,[67] A. Iniukhin,[44] A. Iohner,[10] A. Ishteev,[44] K. Ivshin,[44] H. Jage,[17] S. J. Jaimes Elles,[78,49,50] S. Jakobsen,[50] T. Jakoubek,[79] E. Jans,[38] B. K. Jashal,[49] A. Jawahery,[68] C. Jayaweera,[55] A. Jelavic,[1] V. Jevtic,[19] Z. Jia,[16] E. Jiang,[68] X. Jiang,[5,7] Y. Jiang,[7] Y. J. Jiang,[6] E. Jimenez Moya,[9] N. Jindal,[90] M. John,[65] A. John Rubesh Rajan,[23] D. Johnson,[55] C. R. Jones,[57] S. Joshi,[42] B. Jost,[50] J. Juan Castella,[57] N. Jurik,[50] I. Juszczak,[41] K. Kalecinska,[40] D. Kaminaris,[51] S. Kandybei,[53] M. Kane,[60] Y. Kang,[4,k] C. Kar,[11] M. Karacson,[50] A. Kauniskangas,[51] J. W. Kautz,[67] M. K. Kazanecki,[41] F. Keizer,[50] M. Kenzie,[57] T. Ketel,[38] B. Khanji,[70] A. Kharisova,[44] S. Kholodenko,[63,50] G. Khreich,[14] F. Kiraz,[14] T. Kirn,[17] V. S. Kirsebom,[31,b] S. Klaver,[39] N. Kleijne,[35,i] A. Kleimenova,[51] D. K. Klekots,[87] K. Klimaszewski,[42] M. R. Kmiec,[42] T. Knospe,[19] R. Kolb,[22] S. Koliiev,[54] L. Kolk,[19] A. Konoplyannikov,[6] P. Kopciewicz,[50] P. Koppenburg,[38] A. Korchin,[53] I. Kostiuk,[38] O. Kot,[54] S. Kotriakhova, E. Kowalczyk,[68] A. Kozachuk,[44] P. Kravchenko,[44] L. Kravchuk,[44] O. Kravcov,[82] M. Kreps,[58] P. Krokovny,[44] W. Krupa,[70] W. Krzemien,[42] O. Kshyvanskyi,[54] S. Kubis,[85] M. Kucharczyk,[41] V. Kudryavtsev,[44] E. Kulikova,[44] A. Kupsc,[86] V. Kushnir,[53] B. Kutsenko,[13] J. Kvapil,[69] I. Kyryllin,[53] D. Lacarrere,[50] P. Laguarta Gonzalez,[46] A. Lai,[32] A. Lampis,[32] D. Lancierini,[63] C. Landesa Gomez,[48] J. J. Lane,[1] G. Lanfranchi,[28] C. Langenbruch,[22] J. Langer,[19] T. Latham,[58] F. Lazzari,[35,s] C. Lazzeroni,[55]

R. Le Gac,[13] H. Lee,[62] R. Lefèvre,[11] A. Leflat,[44] S. Legotin,[44] M. Lehuraux,[58] E. Lemos Cid,[50] O. Leroy,[13] T. Lesiak,[41] E. D. Lesser,[50] B. Leverington,[22] A. Li,[4,k] C. Li,[4] C. Li,[13] H. Li,[74] J. Li,[8] K. Li,[77] L. Li,[64] P. Li,[7] P.-R. Li,[75] Q. Li,[5,7] T. Li,[73] T. Li,[74] Y. Li,[8] Y. Li,[5] Y. Li,[4] Z. Lian,[4,k] Q. Liang,[8] X. Liang,[70] Z. Liang,[32] S. Libralon,[49] A. Lightbody,[12] C. Lin,[7] T. Lin,[59] R. Lindner,[50] H. Linton,[63] R. Litvinov,[32] D. Liu,[8] F. L. Liu,[1] G. Liu,[74] K. Liu,[75] S. Liu,[5] W. Liu,[8] Y. Liu,[60] Y. Liu,[75] Y. L. Liu,[63] G. Loachamin Ordonez,[71] I. Lobo,[1] A. Lobo Salvia,[10] A. Loi,[32] T. Long,[57] F. C. L. Lopes,[2,f] J. H. Lopes,[3] A. Lopez Huertas,[46] C. Lopez Iribarnegaray,[48] S. López Soliño,[48] Q. Lu,[15] C. Lucarelli,[50] D. Lucchesi,[33,t] M. Lucio Martinez,[49] Y. Luo,[6] A. Lupato,[33,u] E. Luppi,[26,e] K. Lynch,[23] X.-R. Lyu,[7] G. M. Ma,[4,k] H. Ma,[73] S. Maccolini,[19] F. Machefert,[14] F. Maciuc,[43] B. Mack,[70] I. Mackay,[65] L. M. Mackey,[70] L. R. Madhan Mohan,[57] M. J. Madurai,[55] D. Magdalinski,[38] D. Maisuzenko,[44] J. J. Malczewski,[41] S. Malde,[65] L. Malentacca,[50] A. Malinin,[44] T. Maltsev,[44] G. Manca,[32,m] G. Mancinelli,[13] C. Mancuso,[14] R. Manera Escalero,[46] F. M. Manganella,[37] D. Manuzzi,[25] D. Marangotto,[30,j] J. F. Marchand,[10] R. Marchevski,[51] U. Marconi,[25] E. Mariani,[16] S. Mariani,[50] C. Marin Benito,[46] J. Marks,[22] A. M. Marshall,[56] L. Martel,[65] G. Martelli,[34] G. Martellotti,[36] L. Martinazzoli,[50] M. Martinelli,[31,b] D. Martinez Gomez,[83] D. Martinez Santos,[45] F. Martinez Vidal,[49] A. Martorell i Granollers,[47] A. Massafferri,[2] R. Matev,[50] A. Mathad,[50] V. Matiunin,[44] C. Matteuzzi,[70] K. R. Mattioli,[15] A. Mauri,[63] E. Maurice,[15] J. Mauricio,[46] P. Mayencourt,[51] J. Mazorra de Cos,[49] M. Mazurek,[42] D. Mazzanti Tarancon,[46] M. McCann,[63] N. T. McHugh,[61] A. McNab,[64] R. McNulty,[23] B. Meadows,[67] D. Melnychuk,[42] D. Mendoza Granada,[16] P. Menendez Valdes Perez,[48] F. M. Meng,[4,k] M. Merk,[38,84] A. Merli,[51,30] L. Meyer Garcia,[68] D. Miao,[5,7] H. Miao,[7] M. Mikhasenko,[80] D. A. Milanes,[78,v] A. Minotti,[31,b] E. Minucci,[28] T. Miralles,[11] B. Mitreska,[64] D. S. Mitzel,[19] R. Mocanu,[43] A. Modak,[59] L. Moeser,[19] R. D. Moise,[17] E. F. Molina Cardenas,[88] T. Mombächer,[67] M. Monk,[57] T. Monnard,[51] S. Monteil,[11] A. Morcillo Gomez,[48] G. Morello,[28] M. J. Morello,[35,i] M. P. Morgenthaler,[22] A. Moro,[31,b] J. Moron,[40] W. Morren,[38] A. B. Morris,[82,50] A. G. Morris,[13] R. Mountain,[70] Z. M. Mu,[6] E. Muhammad,[58] F. Muheim,[60] M. Mulder,[38] K. Müller,[52] F. Muñoz-Rojas,[9] V. Mytrochenko,[53] P. Naik,[62] T. Nakada,[51] R. Nandakumar,[59] G. Napoletano,[51] I. Nasteva,[3] M. Needham,[60] E. Nekrasova,[44] N. Neri,[30,j] S. Neubert,[18] N. Neufeld,[50] P. Neustroev,[44] J. Nicolini,[50] D. Nicotra,[84] E. M. Niel,[15] N. Nikitin,[44] L. Nisi,[19] Q. Niu,[75] B. K. Njoki,[50] P. Nogarolli,[3] P. Nogga,[18] C. Normand,[48] J. Novoa Fernandez,[48] G. Nowak,[67] C. Nunez,[88] H. N. Nur,[61] A. Oblakowska-Mucha,[40] V. Obraztsov,[44] T. Oeser,[17] A. Okhotnikov,[44] O. Okhrimenko,[54] R. Oldeman,[32,m] F. Oliva,[60,50] E. Olivart Pino,[46] M. Olocco,[19] R. H. O'Neil,[50] J. S. Ordonez Soto,[11] D. Osthues,[19] J. M. Otalora Goicochea,[3] P. Owen,[52] A. Oyanguren,[49] O. Ozcelik,[50] F. Paciolla,[35,w] A. Padee,[42] K. O. Padeken,[18] B. Pagare,[48] T. Pajero,[50] A. Palano,[24] L. Palini,[30] M. Palutan,[28] C. Pan,[76] X. Pan,[4,k] S. Panebianco,[12] S. Paniskaki,[50,33] G. Panshin,[5] L. Paolucci,[64] A. Papanestis,[59] M. Pappagallo,[24,o] L. L. Pappalardo,[26] C. Pappenheimer,[67] C. Parkes,[64] D. Parmar,[80] G. Passaleva,[27] D. Passaro,[35,i] A. Pastore,[24] M. Patel,[63] J. Patoc,[65] C. Patrignani,[25,g] A. Paul,[70] C. J. Pawley,[84] A. Pellegrino,[38] J. Peng,[5,7] X. Peng,[75] M. Pepe Altarelli,[28] S. Perazzini,[25] D. Pereima,[44] H. Pereira Da Costa,[69] M. Pereira Martinez,[48] A. Pereiro Castro,[48] C. Perez,[47] P. Perret,[11] A. Perrevoort,[83] A. Perro,[50] M. J. Peters,[67] K. Petridis,[56] A. Petrolini,[29,h] S. Pezzulo,[29,h] J. P. Pfaller,[67] H. Pham,[70] L. Pica,[35,i] M. Piccini,[34] L. Piccolo,[32] B. Pietrzyk,[10] G. Pietrzyk,[14] R. N. Pilato,[62] D. Pinci,[36] F. Pisani,[50] M. Pizzichemi,[31,50,b] V. M. Placinta,[43] M. Plo Casasus,[48] T. Poeschl,[50] F. Polci,[16] M. Poli Lener,[28] A. Poluektov,[13] N. Polukhina,[44] I. Polyakov,[64] E. Polycarpo,[3] S. Ponce,[50] D. Popov,[7,50] K. Popp,[19] S. Poslavskii,[44] K. Prasanth,[60] C. Prouve,[45] D. Provenzano,[32,50,m] V. Pugatch,[54] A. Puicercus Gomez,[50] G. Punzi,[35,s] J. R. Pybus,[69] Q. Q. Qian,[6] W. Qian,[7] N. Qin,[4,k] R. Quagliani,[50] R. I. Rabadan Trejo,[58] R. Racz,[82] J. H. Rademacker,[56] M. Rama,[35] M. Ramírez García,[88] V. Ramos De Oliveira,[71] M. Ramos Pernas,[58] M. S. Rangel,[3] F. Ratnikov,[44] G. Raven,[39] M. Rebollo De Miguel,[49] F. Redi,[30,u] J. Reich,[56] F. Reiss,[20] Z. Ren,[7] P. K. Resmi,[65] M. Ribalda Galvez,[46] R. Ribatti,[51] G. Ricart,[12] D. Riccardi,[35,i] S. Ricciardi,[59] K. Richardson,[66] M. Richardson-Slipper,[57] F. Riehn,[19] K. Rinnert,[62] P. Robbe,[14,50] G. Robertson,[61] E. Rodrigues,[62] A. Rodriguez Alvarez,[46] E. Rodriguez Fernandez,[48] J. A. Rodriguez Lopez,[78] E. Rodriguez Rodriguez,[50] J. Roensch,[19] A. Rogachev,[44] A. Rogovskiy,[59] D. L. Rolf,[19] P. Roloff,[50] V. Romanovskiy,[67] A. Romero Vidal,[48] G. Romolini,[26,50] F. Ronchetti,[51] T. Rong,[6] M. Rotondo,[28] M. S. Rudolph,[70] M. Ruiz Diaz,[22] R. A. Ruiz Fernandez,[48] J. Ruiz Vidal,[84] J. J. Saavedra-Arias,[9]

J. J. Saborido Silva,[48] S. E. R. Sacha Emile R.,[50] N. Sagidova,[44] D. Sahoo,[81] N. Sahoo,[55] B. Saitta,[32] M. Salomoni,[31,50,b] I. Sanderswood,[49] R. Santacesaria,[36] C. Santamarina Rios,[48] M. Santimaria,[28] L. Santoro,[2] E. Santovetti,[37] A. Saputi,[26,50] D. Saranin,[44] A. Sarnatskiy,[83] G. Sarpis,[50] M. Sarpis,[82] C. Satriano,[36] A. Satta,[37] M. Saur,[75] D. Savrina,[44] H. Sazak,[17] F. Sborzacchi,[50,28] A. Scarabotto,[19] S. Schael,[17] S. Scherl,[62] M. Schiller,[22] H. Schindler,[50] M. Schmelling,[21] B. Schmidt,[50] N. Schmidt,[69] S. Schmitt,[66] H. Schmitz,[18] O. Schneider,[51] A. Schopper,[63] N. Schulte,[19] M. H. Schune,[14] G. Schwering,[17] B. Sciascia,[28] A. Sciuccati,[50] G. Scriven,[84] I. Segal,[80] S. Sellam,[48] A. Semennikov,[44] T. Senger,[52] M. Senghi Soares,[39] A. Sergi,[29,h] N. Serra,[52] L. Sestini,[27] B. Sevilla Sanjuan,[47] Y. Shang,[6] D. M. Shangase,[88] M. Shapkin,[44] R. S. Sharma,[70] I. Shchemerov,[44] L. Shchutska,[51] T. Shears,[62] L. Shekhtman,[44] Z. Shen,[38] S. Sheng,[51] V. Shevchenko,[44] B. Shi,[7] J. Shi,[57] Q. Shi,[7] W. S. Shi,[74] Y. Shimizu,[14] E. Shmanin,[25] R. Shorkin,[44] R. Silva Coutinho,[2] G. Simi,[33,t] S. Simone,[24,o] M. Singha,[81] I. Siral,[51] N. Skidmore,[58] T. Skwarnicki,[70] M. W. Slater,[55] E. Smith,[66] M. Smith,[63] L. Soares Lavra,[60] M. D. Sokoloff,[67] F. J. P. Soler,[61] A. Solomin,[56] A. Solovev,[44] K. Solovieva,[20] N. S. Sommerfeld,[18] R. Song,[1] Y. Song,[51] Y. Song,[4,k] Y. S. Song,[6] F. L. Souza De Almeida,[46] B. Souza De Paula,[3] K. M. Sowa,[40] E. Spadaro Norella,[29,h] E. Spedicato,[25] J. G. Speer,[19] P. Spradlin,[61] F. Stagni,[50] M. Stahl,[80] S. Stahl,[50] S. Stanislaus,[65] M. Stefaniak,[90] O. Steinkamp,[52] D. Strekalina,[44] Y. Su,[7] F. Suljik,[65] J. Sun,[32] J. Sun,[64] L. Sun,[76] D. Sundfeld,[2] W. Sutcliffe,[52] P. Svihra,[79] V. Svintozelskyi,[49] K. Swientek,[40] F. Swystun,[57] A. Szabelski,[42] T. Szumlak,[40] Y. Tan,[4] Y. Tang,[76] Y. T. Tang,[7] M. D. Tat,[22] J. A. Teijeiro Jimenez,[48] A. Terentev,[44] F. Terzuoli,[35,w] F. Teubert,[50] E. Thomas,[50] D. J. D. Thompson,[55] A. R. Thomson-Strong,[60] H. Tilquin,[63] V. Tisserand,[11] S. T'Jampens,[10] M. Tobin,[5,50] T. T. Todorov,[20] L. Tomassetti,[26,e] G. Tonani,[30] X. Tong,[6] T. Tork,[30] L. Toscano,[19] D. Y. Tou,[4,k] C. Trippl,[47] G. Tuci,[22] N. Tuning,[38] L. H. Uecker,[22] A. Ukleja,[40] D. J. Unverzagt,[22] A. Upadhyay,[50] B. Urbach,[60] A. Usachov,[38] A. Ustyuzhanin,[44] U. Uwer,[22] V. Vagnoni,[25,50] A. Vaitkevicius,[82] V. Valcarce Cadenas,[48] G. Valenti,[25] N. Valls Canudas,[50] J. van Eldik,[50] H. Van Hecke,[69] E. van Herwijnen,[63] C. B. Van Hulse,[48,x] R. Van Laak,[51] M. van Veghel,[84] G. Vasquez,[52] R. Vazquez Gomez,[46] P. Vazquez Regueiro,[48] C. Vázquez Sierra,[45] S. Vecchi,[26] J. Velilla Serna,[49] J. J. Velthuis,[56] M. Veltri,[27,y] A. Venkateswaran,[51] M. Verdoglia,[32] M. Vesterinen,[58] W. Vetens,[70] D. Vico Benet,[65] P. Vidrier Villalba,[46] M. Vieites Diaz,[48] X. Vilasis-Cardona,[47] E. Vilella Figueras,[62] A. Villa,[25] P. Vincent,[16] B. Vivacqua,[3] F. C. Volle,[55] D. vom Bruch,[13] N. Voropaev,[44] K. Vos,[84] C. Vrahas,[60] J. Wagner,[19] J. Walsh,[35] E. J. Walton,[1] G. Wan,[6] A. Wang,[7] B. Wang,[5] C. Wang,[22] G. Wang,[8] H. Wang,[75] J. Wang,[7] J. Wang,[5] J. Wang,[4,k] J. Wang,[76] M. Wang,[50] N. W. Wang,[7] R. Wang,[56] X. Wang,[8] X. Wang,[74] X. W. Wang,[63] Y. Wang,[77] Y. Wang,[6] Y. H. Wang,[75] Z. Wang,[14] Z. Wang,[30] J. A. Ward,[58,1] M. Waterlaat,[50] N. K. Watson,[55] D. Websdale,[63] Y. Wei,[6] Z. Weida,[7] J. Wendel,[45] B. D. C. Westhenry,[56] C. White,[57] M. Whitehead,[61] E. Whiter,[55] A. R. Wiederhold,[64] D. Wiedner,[19] M. A. Wiegertjes,[38] C. Wild,[65] G. Wilkinson,[65,50] M. K. Wilkinson,[67] M. Williams,[66] M. J. Williams,[50] M. R. J. Williams,[60] R. Williams,[57] S. Williams,[56] Z. Williams,[56] F. F. Wilson,[59] M. Winn,[12] W. Wislicki,[42] M. Witek,[41] L. Witola,[19] T. Wolf,[22] E. Wood,[57] G. Wormser,[14] S. A. Wotton,[57] H. Wu,[70] J. Wu,[8] X. Wu,[76] Y. Wu,[6,57] Z. Wu,[7] K. Wyllie,[50] S. Xian,[74] Z. Xiang,[5] Y. Xie,[8] T. X. Xing,[30] A. Xu,[35,i] L. Xu,[4,k] M. Xu,[50] Z. Xu,[50] Z. Xu,[7] Z. Xu,[5] S. Yadav,[26] K. Yang,[63] X. Yang,[6] Y. Yang,[7] Y. Yang,[81] Z. Yang,[6] H. Yeung,[64] H. Yin,[8] X. Yin,[7] C. Y. Yu,[6] J. Yu,[73] X. Yuan,[5] Y Yuan,[5,7] J. A. Zamora Saa,[72] M. Zavertyaev,[21] M. Zdybal,[41] F. Zenesini,[25] C. Zeng,[5,7] M. Zeng,[4,k] C. Zhang,[6] D. Zhang,[8] J. Zhang,[7] L. Zhang,[4,k] R. Zhang,[8] S. Zhang,[65] S. L. Zhang,[73] Y. Zhang,[6] Y. Z. Zhang,[4,k] Z. Zhang,[4,k] Y. Zhao,[22] A. Zhelezov,[22] S. Z. Zheng,[6] X. Z. Zheng,[4,k] Y. Zheng,[7] T. Zhou,[6] X. Zhou,[8] V. Zhovkovska,[58] L. Z. Zhu,[7] X. Zhu,[4,k] X. Zhu,[8] Y. Zhu,[17] V. Zhukov,[17] J. Zhuo,[49] D. Zuliani,[33,t] and G. Zunica[28]

(LHCb Collaboration)

[1]*School of Physics and Astronomy, Monash University, Melbourne, Australia*
[2]*Centro Brasileiro de Pesquisas Físicas (CBPF), Rio de Janeiro, Brazil*
[3]*Universidade Federal do Rio de Janeiro (UFRJ), Rio de Janeiro, Brazil*
[4]*Department of Engineering Physics, Tsinghua University, Beijing, China*

[5]Institute Of High Energy Physics (IHEP), Beijing, China
[6]School of Physics State Key Laboratory of Nuclear Physics and Technology, Peking University, Beijing, China
[7]University of Chinese Academy of Sciences, Beijing, China
[8]Institute of Particle Physics, Central China Normal University, Wuhan, Hubei, China
[9]Consejo Nacional de Rectores (CONARE), San Jose, Costa Rica
[10]Université Savoie Mont Blanc, CNRS, IN2P3-LAPP, Annecy, France
[11]Université Clermont Auvergne, CNRS/IN2P3, LPC, Clermont-Ferrand, France
[12]Université Paris-Saclay, Centre d'Etudes de Saclay (CEA), IRFU, Saclay, France
[13]Aix Marseille Univ, CNRS/IN2P3, CPPM, Marseille, France
[14]Université Paris-Saclay, CNRS/IN2P3, IJCLab, Orsay, France
[15]Laboratoire Leprince-Ringuet, CNRS/IN2P3, Ecole Polytechnique, Institut Polytechnique de Paris, Palaiseau, France
[16]Laboratoire de Physique Nucléaire et de Hautes Énergies (LPNHE), Sorbonne Université, CNRS/IN2P3, F-75005 Paris, France
[17]I. Physikalisches Institut, RWTH Aachen University, Aachen, Germany
[18]Universität Bonn—Helmholtz-Institut für Strahlen und Kernphysik, Bonn, Germany
[19]Fakultät Physik, Technische Universität Dortmund, Dortmund, Germany
[20]Physikalisches Institut, Albert-Ludwigs-Universität Freiburg, Freiburg, Germany
[21]Max-Planck-Institut für Kernphysik (MPIK), Heidelberg, Germany
[22]Physikalisches Institut, Ruprecht-Karls-Universität Heidelberg, Heidelberg, Germany
[23]School of Physics, University College Dublin, Dublin, Ireland
[24]INFN Sezione di Bari, Bari, Italy
[25]INFN Sezione di Bologna, Bologna, Italy
[26]INFN Sezione di Ferrara, Ferrara, Italy
[27]INFN Sezione di Firenze, Firenze, Italy
[28]INFN Laboratori Nazionali di Frascati, Frascati, Italy
[29]INFN Sezione di Genova, Genova, Italy
[30]INFN Sezione di Milano, Milano, Italy
[31]INFN Sezione di Milano-Bicocca, Milano, Italy
[32]INFN Sezione di Cagliari, Monserrato, Italy
[33]INFN Sezione di Padova, Padova, Italy
[34]INFN Sezione di Perugia, Perugia, Italy
[35]INFN Sezione di Pisa, Pisa, Italy
[36]INFN Sezione di Roma La Sapienza, Roma, Italy
[37]INFN Sezione di Roma Tor Vergata, Roma, Italy
[38]Nikhef National Institute for Subatomic Physics, Amsterdam, Netherlands
[39]Nikhef National Institute for Subatomic Physics and VU University Amsterdam, Amsterdam, Netherlands
[40]AGH—University of Krakow, Faculty of Physics and Applied Computer Science, Kraków, Poland
[41]Henryk Niewodniczanski Institute of Nuclear Physics Polish Academy of Sciences, Kraków, Poland
[42]National Center for Nuclear Research (NCBJ), Warsaw, Poland
[43]Horia Hulubei National Institute of Physics and Nuclear Engineering, Bucharest-Magurele, Romania
[44]Authors affiliated with an institute formerly covered by a cooperation agreement with CERN
[45]Universidade da Coruña, A Coruña, Spain
[46]ICCUB, Universitat de Barcelona, Barcelona, Spain
[47]La Salle, Universitat Ramon Llull, Barcelona, Spain
[48]Instituto Galego de Física de Altas Enerxías (IGFAE), Universidade de Santiago de Compostela, Santiago de Compostela, Spain
[49]Instituto de Fisica Corpuscular, Centro Mixto Universidad de Valencia—CSIC, Valencia, Spain
[50]European Organization for Nuclear Research (CERN), Geneva, Switzerland
[51]Institute of Physics, Ecole Polytechnique Fédérale de Lausanne (EPFL), Lausanne, Switzerland
[52]Physik-Institut, Universität Zürich, Zürich, Switzerland
[53]NSC Kharkiv Institute of Physics and Technology (NSC KIPT), Kharkiv, Ukraine
[54]Institute for Nuclear Research of the National Academy of Sciences (KINR), Kyiv, Ukraine
[55]School of Physics and Astronomy, University of Birmingham, Birmingham, United Kingdom
[56]H.H. Wills Physics Laboratory, University of Bristol, Bristol, United Kingdom
[57]Cavendish Laboratory, University of Cambridge, Cambridge, United Kingdom
[58]Department of Physics, University of Warwick, Coventry, United Kingdom
[59]STFC Rutherford Appleton Laboratory, Didcot, United Kingdom
[60]School of Physics and Astronomy, University of Edinburgh, Edinburgh, United Kingdom
[61]School of Physics and Astronomy, University of Glasgow, Glasgow, United Kingdom
[62]Oliver Lodge Laboratory, University of Liverpool, Liverpool, United Kingdom
[63]Imperial College London, London, United Kingdom
[64]Department of Physics and Astronomy, University of Manchester, Manchester, United Kingdom

[65]Department of Physics, University of Oxford, Oxford, United Kingdom
[66]Massachusetts Institute of Technology, Cambridge, Massachusetts, USA
[67]University of Cincinnati, Cincinnati, Ohio, USA
[68]University of Maryland, College Park, Maryland, USA
[69]Los Alamos National Laboratory (LANL), Los Alamos, New Mexico, USA
[70]Syracuse University, Syracuse, New York, USA
[71]Pontifícia Universidade Católica do Rio de Janeiro (PUC-Rio), Rio de Janeiro, Brazil
(associated with Universidade Federal do Rio de Janeiro (UFRJ), Rio de Janeiro, Brazil)
[72]Universidad Andres Bello, Santiago, Chile (associated with Physik-Institut, Universität Zürich, Zürich, Switzerland)
[73]School of Physics and Electronics, Hunan University, Changsha City, China
(associated with Institute of Particle Physics, Central China Normal University, Wuhan, Hubei, China)
[74]State Key Laboratory of Nuclear Physics and Technology, South China Normal University, Guangzhou, China
(associated with Department of Engineering Physics, Tsinghua University, Beijing, China)
[75]Lanzhou University, Lanzhou, China (associated with Institute Of High Energy Physics (IHEP), Beijing, China)
[76]School of Physics and Technology, Wuhan University, Wuhan, China
(associated with Department of Engineering Physics, Tsinghua University, Beijing, China)
[77]Henan Normal University, Xinxiang, China
(associated with Institute of Particle Physics, Central China Normal University, Wuhan, Hubei, China)
[78]Departamento de Fisica, Universidad Nacional de Colombia, Bogota, Colombia
(associated with Laboratoire de Physique Nucléaire et de Hautes Énergies (LPNHE),
Sorbonne Université, CNRS/IN2P3, F-75005 Paris, France)
[79]Institute of Physics of the Czech Academy of Sciences, Prague, Czech Republic
(associated with Department of Physics and Astronomy, University of Manchester,
Manchester, United Kingdom)
[80]Ruhr Universitaet Bochum, Fakultaet f. Physik und Astronomie, Bochum, Germany
(associated with Fakultät Physik, Technische Universität Dortmund, Dortmund, Germany)
[81]Eotvos Lorand University, Budapest, Hungary
(associated with European Organization for Nuclear Research (CERN), Geneva, Switzerland)
[82]Faculty of Physics, Vilnius University, Vilnius, Lithuania
(associated with Physikalisches Institut, Albert-Ludwigs-Universität Freiburg, Freiburg, Germany)
[83]Van Swinderen Institute, University of Groningen, Groningen, Netherlands
(associated with Nikhef National Institute for Subatomic Physics, Amsterdam, Netherlands)
[84]Universiteit Maastricht, Maastricht, Netherlands
(associated with Nikhef National Institute for Subatomic Physics, Amsterdam, Netherlands)
[85]Tadeusz Kosciuszko Cracow University of Technology, Cracow, Poland
(associated with Henryk Niewodniczanski Institute of Nuclear Physics Polish Academy of Sciences, Kraków, Poland)
[86]Department of Physics and Astronomy, Uppsala University, Uppsala, Sweden
(associated with School of Physics and Astronomy, University of Glasgow, Glasgow, United Kingdom)
[87]Taras Schevchenko University of Kyiv, Faculty of Physics, Kyiv, Ukraine
(associated with Université Paris-Saclay, CNRS/IN2P3, IJCLab, Orsay, France)
[88]University of Michigan, Ann Arbor, Michigan, USA (associated with Syracuse University, Syracuse, New York, USA)
[89]Indiana University, Bloomington, Indiana, USA
(associated with Los Alamos National Laboratory (LANL), Los Alamos, New Mexico, USA)
[90]Ohio State University, Columbus, Ohio, USA
(associated with Los Alamos National Laboratory (LANL), Los Alamos, New Mexico, USA)

[a]Also at Lamarr Institute for Machine Learning and Artificial Intelligence, Dortmund, Germany.
[b]Also at Università degli Studi di Milano-Bicocca, Milano, Italy.
[c]Also at Università di Modena e Reggio Emilia, Modena, Italy.
[d]Also at Department of Physics and Astronomy, University of Victoria, Victoria, Canada.
[e]Also at Università di Ferrara, Ferrara, Italy.
[f]Also at Universidade Estadual de Campinas (UNICAMP), Campinas, Brazil.
[g]Also at Università di Bologna, Bologna, Italy.
[h]Also at Università di Genova, Genova, Italy.
[i]Also at Scuola Normale Superiore, Pisa, Italy.
[j]Also at Università degli Studi di Milano, Milano, Italy.
[k]Also at Center for High Energy Physics, Tsinghua University, Beijing, China.
[l]Also at Universidad Nacional Autónoma de Honduras, Tegucigalpa, Honduras.
[m]Also at Università di Cagliari, Cagliari, Italy.
[n]Also at Centro Federal de Educacão Tecnológica Celso Suckow da Fonseca, Rio De Janeiro, Brazil.

[o]Also at Università di Bari, Bari, Italy.
[p]Also at Università di Perugia, Perugia, Italy.
[q]Also at LIP6, Sorbonne Université, Paris, France.
[r]Also at Hangzhou Institute for Advanced Study, UCAS, Hangzhou, China.
[s]Also at Università di Pisa, Pisa, Italy.
[t]Also at Università di Padova, Padova, Italy.
[u]Also at Università di Bergamo, Bergamo, Italy.
[v]Also at Universidad de Ingeniería y Tecnología (UTEC), Lima, Peru.
[w]Also at Università di Siena, Siena, Italy.
[x]Also at Universidad de Alcalá, Alcalá de Henares, Spain.
[y]Also at Università di Urbino, Urbino, Italy.